PERGAMON

Available online at www.sciencedirect.com

SCIENCE DIRECT®

Polyhedron 22 (2003) 177–188

POLYHEDRON

www.elsevier.com/locate/poly

Octamolybdate subunits as building blocks in the hydrothermal synthesis of organically templated mixed metal oxides: the synthesis and X-ray characterization of $[Cu_2Mo_4O_{13}(3,3'\text{-bipy})_2]\cdot H_2O$, $[CuMo_4O_{13}(Hdipyreth)]$, and $[Cu(dpp)]_2[Cu_2(\alpha\text{-}Mo_8O_{26})(dpp)_2]\cdot 2H_2O$ (3,3′-bipy = 3,3′-bipyridine; dipyreth = 1,2-bis(2-pyridyl)ethylene; dpp = 4,4′-trimethylenedipyridine)

Randy S. Rarig, Jr., Jon Zubieta *

Department of Chemistry, Syracuse University, Syracuse, NY 13244, USA

Received 5 August 2002; accepted 27 September 2002

Dedicated to Professor Pierre Gouzerh on the occasion of his 60th birthday.

Abstract

The hydrothermal reactions of MoO_3, an appropriate Cu(II) source, and a dipodal nitrogen donor ligand yielded a series of bimetallic oxides $[Cu_2Mo_4O_{13}(3,3'\text{-bipy})_2]\cdot H_2O$ (**1**·H_2O), $[CuMo_4O_{13}(Hdipyreth)]$ (**2**), and $[Cu(dpp)]_2[Cu_2(\alpha\text{-}Mo_8O_{26})(dpp)_2]\cdot 2H_2O$ (**3**·$2H_2O$). (3,3′-bipy = 3,3′-bipyridine; dipyreth = 1,2-bis(2-pyridyl)ethylene; dpp = 4,4′-trimethylenedipyridine). The materials **1**·H_2O and **2** are constructed from octamolybdate clusters linked through copper-ligand subunits, while **3**·$2H_2O$ exhibits fused octamolybdate building blocks in a two-dimensional molybdate chain.

Keywords: Octamolybdate subunits; Hydrothermal synthesis; Mixed metal oxides; Hydrothermal reactions

1. Introduction

The contemporary interest in the applications of supramolecular chemistry to solid state inorganic chemistry [1] reflects the need for rational design of functional materials [2]. One strategy for the development of synthetic routes for crystal engineering of materials exploits multitopic organic spacer ligands, which have provided a number of diverse topologies [3–5]. The prototypical materials of this class are polymeric coordination complex cations constructed from Cu[I], Ag[I], Cu[II], Zn[II], and Cd[II] centers and organodiimine bridging ligands [6,7]. In an extrapolation of this general approach, we have recently demonstrated that organic–inorganic composite materials constructed of molybdenum oxide, a divalent secondary transition metal and organodiamine substructures may be prepared through hydrothermal synthetic routes. As part of our general investigations of the structure directing roles of organic subunits on the microstructures of hybrid oxide materials [8–10], we have exploited molecular molybdenum oxide clusters as building blocks, linked

* Corresponding author. Tel.: +1-315-443-2925; fax: +1-315-443-4070

E-mail address: jazubiet@syr.edu (J. Zubieta).

0277-5387/02/$ - see front matter
PII: S0277-5387(02)01268-8

either through direct coordination into oxo-bridged arrays of clusters or through secondary metal sites acting as bridging coordination complex subunits [11–13]. This approach is quite general and has been described for polyoxoanion clusters, other than molybdates [14]. Furthermore, the linking of polyoxometalate clusters into supramolecular materials is also manifested in the molecular growth of clusters [15]. In this contribution, we describe the synthesis and structure of the organic–inorganic hybrid materials $[Cu_2Mo_4O_{13}(3\text{-}3'\text{-bipy})_2]\cdot H_2O$ (**1**·H_2O), $[CuMo_4O_{13}(Hdipyreth)]$ (**2**), and $[Cu(dpp)]_2[Cu_2(\alpha\text{-}Mo_8O_{26})(dpp)_2]\cdot 2H_2O$ (**3**·$2H_2O$).

2. Experimental

2.1. Synthesis of 3,3′-bipyridine (3,3′-bpy)

All manipulations were carried out under an atmosphere of dry nitrogen. Trimethyltin chloride (50 g) was dissolved in 50 ml of ethylene glycol dimethylether (dme). This solution was added dropwise with stirring over a period of 20 min to a solution of sodium (18 g) in dme (200 ml) in a 500 ml round bottom flask in a salt–ice bath at −10 °C.

After 2 h of stirring, the solution turned dark green. The round bottom flask was then transferred to a glove box; the mixture was filtered through a course funnel and transferred to another 500 ml round bottom flask. The 500 ml round bottom flask was then taken from the glove box and placed back on an Schlenk line. 3-Bromopyridine (20 g) dissolved in 150 ml of dimethoxy ethane was added dropwise to the solution in an ice–salt bath and stirred for 3 h to yield a yellow solution. The solvent was then removed under vacuum at room temperature to produce a thick yellow paste. Ether (250 ml) was added to the paste, and the solution was filtered in a glove box to remove the NaBr by-product. The solution was then returned to the Schlenk line, whereupon ether was removed under vacuum to produce a yellow/orange paste, which was then distilled through a short path distillation apparatus to yield two fractions. The second fraction of 3-trimethylstannyl pyridine, which distilled at 45 °C, was collected for further use.

The clear solution of 3-trimethylstannyl pyridine was refluxed for 12 h in freshly distilled xylene (1 l), containing tetrakistriphenylphosphine palladium(0) (2.4 g), and 3-bromopyridine (30 g). The solution turned yellow upon mixing, and then dark green upon refluxing. After cooling, a dark green solid precipitated to leave a light yellow solution. The solution was extracted with 15% HCl. The aqueous layer was collected and extracted with ether (500 ml in 100 ml portions). The aqueous layer was collected and NaOH added to pH 8.0, whereupon the solution turned orange. The orange solution was washed with chloroform, dried over sodium sulfate, and gravity filtered. Solvent removal in vacuo yielded a yellow paste, which was eluted through an alumina column in ether. The ether was removed in vacuo, and the resulting paste was distilled in a short path distillation apparatus to yield the product at 98 °C.

2.2. Synthesis of $[Cu_2Mo_4O_{13}(3,3'\text{-bipy})_2]\cdot H_2O$ (**1**·H_2O)

A mixture of $CuCl_2\cdot 2H_2O$ (0.094 g, 0.54 mmol), MoO_3 (0.079 g, 0.54 mmol), 3,3′-bipyridine (0.07 g, 0.54 mmol), H_2O (10.0 g, 0.56 mol) and sufficient 20% $(C_4H_9)_4NOH$ to adjust the pH to 7.2 was heated to 180 °C for 75 h, whereupon orange crystals of **1** were isolated in 20% yield based on Mo.

2.3. Synthesis of $[CuMo_4O_{13}(Hdipyreth)]$ (**2**)

A mixture of $CuSO_4\cdot 5H_2O$ (0.119 g, 0.48 mmol), MoO_3 (0.048 g, 0.33 mmol), 1,2-bis(2-pyridyl)ethylene (0.04 g, 0.22 mmol), H_2O (10.0 g, 0.56 mol) was heated to 120 °C for 76.5 h, whereupon orange crystals of **2** were isolated in 40% yield based on Mo.

2.4. Synthesis of $[Cu(dpp)]_2[Cu_2(\alpha\text{-}Mo_8O_{26})(dpp)_2]\cdot 2H_2O$ (**3**·$2H_2O$)

A mixture of $CuSO_4\cdot 5H_2O$ (0.046 g, 0.19 mmol), MoO_3 (0.027 g, 0.19 mmol), 4,4′-trimethylenedipyridine (0.055 g, 0.28 mmol), H_2O (10.0 g, 0.56 mol) was heated to 120 °C for 48 h, whereupon orange crystals of **3** were isolated in 30% yield based on Mo.

2.5. X-ray structural studies

Structural measurements for **1**–**3** were performed on a Bruker SMART-CCD [16] diffractometer at a temperature of 90 ± 1 K using graphite monochromated Mo Kα radiation (λ(Mo Kα) = 0.71073 Å). The data were corrected for Lorentz and polarization effects and absorption using SADABS [17]. The structures were solved by direct methods. In all cases, all non-hydrogen atoms were refined anistropically. After locating all of the non-hydrogen atoms, the models were refined against F^2, initially using isotropic and later anisotropic thermal displacement parameters until the final values of Δ/σ_{max} were less than 0.001 in all cases. Hydrogen atoms were introduced in calculated positions and refined isotropically. Neutral atom scattering coefficients and anomalous dispersion corrections were taken from the International Tables, Volume C. All calculations were performed using the SHELXTL [18] crystallographic software packages.

Table 1
Selected structural parameters for octamolybdate isomers

Compound	Tetrahedral sites		Square pyramidal sites		Octaheral sites		Number of oxo-group types				
	Number	Mo–O (type)	Number	Mo–O (type)	Number	Mo–O (type)	O_t	μ_2-O	μ_3-O	μ_4-O	μ_5-O
$[\{Cu(bpp)\}_2\{Cu_2(\alpha\text{-}Mo_8O_{26})(dpp)_2\}\cdot 2H_2O$	2	1.724(8)(O_t), 1.789(8)($\mu_3 \times 3$)			6	1.705(9)($O_t \times 2$), 1.908(9)($\mu_2 \times 2$), 2.435(9)($\mu_3 \times 2$)	14	6	6		
$[\{Cu_4(\beta\text{-}Mo_8O_{26})(3,3\text{-bipy})_4\}]\cdot 2H_2O$					2, type 1	1.702(4)($O_t \times 2$), 1.924(4)($\mu_2 \times 2$), 2.317(4)($\mu_2 \times 1$), 2.423(3)($\mu_5 \times 1$)	14	6	4		2
					4, type 2	1.704(4)($O_t \times 2$), 1.893(4)($\mu_2 \times 1$), 1.956(4)($\mu_3 \times 1$), 2.326(4)($\mu_3 \times 1$), 2.344(4)($\mu_5 \times 1$)					
					2, type 3	1.691(4)($O_t \times 1$), 1.753(4)($\mu_2 \times 1$), 1.954(4)($\mu_3 \times 2$), 2.274(4)($\mu_5 \times 2$)					
$[Me_3N(CH_2)_6Nme_3]_2[\delta\text{-}Mo_8O_{26}]$			2	1.701(5)($O_t \times 2$), 1.829(5)($\mu_2 \times 1$), 1.893(4)($\mu_3 \times 1$), 2.356(5)($\mu_3 \times 1$)	2, type 1	1.694(4)($O_t \times 1$), 1.747(5)($\mu_2 \times 1$), 1.881(4)($\mu_3 \times 1$), 2.291(5)($\mu_3 \times 1$), 1.907(4)($\mu_4 \times 1$), 2.494(4)($\mu_4 \times 1$)	14	6	4	2	-
					2, type 2	1.701(4)($O_t \times 2$), 1.900(4)($\mu_2 \times 1$), 2.368(4)($\mu_2 \times 1$), 2.173(4)($\mu_3 \times 2$)					
					2, type 3	1.697(5)($O_t \times 2$), 1.961(5)($\mu_2 \times 2$), 2.154(4)($\mu_3 \times 1$), 2.495(4)($\mu_4 \times 1$)					
$(H_3tptz)[\delta\text{-}Mo_8O_{26}]\cdot 2H_2O$	2, type 1	1.708(2)($O_t \times 2$), 1.839(2)($\mu_2 \times 2$)			4	1.699(2)($O_t \times 2$), 1.964(2)($\mu_2 \times 2$), 2.262(2)($\mu_2 \times 1$)	14	10	2		
	2, type 2	1.709(3)($O_t \times 1$), 1.778(2)($\mu_2 \times 2$), 1.855(3)($\mu_3 \times 1$), [2.655(2)($\mu_{3,4} \times 1$)]									
$[(RhCp^*)_2(\mu_2\text{-}SCH_3)_3]_4[\delta\text{-}Mo_8O_{26}]$	2, type 1	1.689($O_t \times 2$), 1.831($\mu_2 \times 2$), [2.730($\mu_{2,3} \times 1$)]			4	1.698($O_t \times 2$), 1.936($\mu_2 \times 2$), 2.308($\mu_2 \times 1$), 2.350($\mu_3 \times 1$)	14	10	2		
	2, type 2	1.698($O_t \times 1$), 1.770($\mu_2 \times 2$), 1.836($\mu_3 \times 1$), [2.878($\mu_{3,4} \times 1$)]									
$[\{Cu(4,4'\text{-bpy})\}_4(\delta\text{-}Mo_8O_{26})]$	2, type 1	1.704(2)($O_t \times 2$), 1.837(2) ($\mu_2 \times 2$), [2.654(5)($\mu_{2,3} \times 1$)			2, type 1	1.706(5)($O_t \times 2$), 1.883(4)($\mu_2 \times 1$), 1.982(4)($\mu_2 \times 1$), 2.222(4)($\mu_3 \times 1$), 2.447(5)($\mu_2 \times 1$)	14	10	2		
	2, type 2	1.723(6)($O_t \times 1$), 1.765(6)($\mu_2 \times 2$), 1.846(4)($\mu_3 \times 1$), [2.825(4)($\mu_{3,4} \times 1$)]			2, type 2	1.688(5)($O_t \times 2$), 1.953(5)($\mu_2 \times 2$), 2.266(5)($\mu_2 \times 1$), 2.422(4)($\mu_3 \times 1$)					
$[\{Ni(H_2O)_2(4,4'\text{-bpy})_2\}_2(\varepsilon\text{-}Mo_8O_{26})]$			2, type 1	1.717(6)($O_t \times 2$), 1.877(6)($\mu_3 \times 2$), 2.206(6)($\mu_3 \times 1$)	2	1.694(5)($O_t \times 2$), 1.939(6)($\mu_2 \times 2$), 2.342(6)($\mu_3 \times 2$)	16	4	6		

Table 1 (*Continued*)

Compound	Tetrahedral sites		Square pyramidal sites		Octaheral sites		Number of oxo-group types				
	Number	Mo–O (type)	Number	Mo–O (type)	Number	Mo–O (type)	O_t	μ_2-O	μ_3-O	μ_4-O	μ_5-O
			4, type 2	1.709(6)($O_t \times 2$), 1.902(6)($\mu_2 \times 1$), 2.060(6)($\mu_3 \times 2$)							
[{Ni(phen)$_2$}$_2$(ξ-Mo_8O_{26})]			2, type 1	1.709(9)($O_t \times 2$), 1.830(10)($\mu_2 \times 1$), 1.894(9)($\mu_3 \times 1$), 2.244(8)($\mu_3 \times 1$)	2, type 1	1.723(9)($O_t \times 2$), 1.876(9)($\mu_2 \times 1$), 2.341(9)($\mu_2 \times 1$), 2.089(10)($\mu_3 \times 2$)	14	6	6		
			2, type 2	1.688(9)($O_t \times 2$), 1.979(9)($\mu_2 \times 2$), 2.182(9)($\mu_3 \times 1$)	2, type 2	1.694(10)($O_t \times 1$), 1.734(8)($\mu_2 \times 1$), 1.915(10)($\mu_3 \times 3$), 2.197(8)($\mu_3 \times 1$)					

Crystallographic details for the structures of **1**–**3** are summarized in Table 2. Atomic positional parameters, full tables of bond lengths and angles and anisotropic temperature factors are available in the Supplementary Tables. Selected bond lengths and angles for **1**–**3** are given in Tables 3–5, respectively.

3. Discussion

Hydrothermal methods are well established in the synthesis of zeolites [19], and more recently in the synthesis of materials of the oxomolybdenum–phosphate [20], oxovanadium–phosphate and organophosphonate systems [21]. Hydrothermal reactions, typically carried out in the temperature range 110–260 °C under autogenous pressure, exploit the self-assembly of the product from soluble precursors. The reduced viscosity of the solvent under these conditions results in enhanced rates of solvent extraction of solids and crystal growth from solution. Since differential solubility problems are minimized, a variety of simple starting materials may be introduced, as well as a number of organic and/or inorganic structure directing (templating) agents from which those of appropriate shape(s) and size(s) may be selected for efficient crystal packing during the crystallization process. Under such nonequilibrium crystallization conditions, metastable

Table 2
Crystal data for compounds **1**·H_2O, **2**, and **3**·$2H_2O$

	[$Cu_2Mo_4O_{13}$(3,3′-bipy)$_2$]·H_2O	[$CuMo_4O_{13}$(Hdipyreth)]	[{Cu(dpp)}$_2${Cu_2(α-Mo_8O_{26})(dpp)$_2$}]·$2H_2O$
Empirical formula	$C_{10}H_9CuMo_2N_2O_7$	$C_{12}H_{10}CuMo_4N_2O_{13}$	$C_{13}H_{15}CuMo_2N_2O_7$
Formula weight	524.61	837.52	566.69
Crystal system	monoclinic	triclinic	Triclinic
Space group	*C*2/*m*	$P\bar{1}$	$P\bar{1}$
a (Å)	13.5238(9)	8.2925(7)	10.6115(7)
b (Å)	21.181(2)	10.8284(9)	13.3836(9)
c (Å)	10.1846(7)	12.412(1)	13.480(1)
α (°)		110.392(1)	94.770(2)
β (°)	115.848(1)	106.603(1)	110.577(1)
γ (°)		97.086(1)	103.443(1)
V (Å^3)	2625.5(3)	969.8(1)	1714.4(2)
Z	8	2	2
D_{calc} (g cm^{-3})	2.654	2.868	1.098
μ (cm^{-1})	35.25	36.68	13.54
λ Mo Kα	0.7103	0.7103	0.7103
R_1 [a]	0.12	0.0656	0.1602
wR_2 [b]	0.1106	0.1053	0.1724

[a] $\Sigma(|F_o|-|F_c|)/\Sigma(|F_o|$.
[b] $[\Sigma[w(F_o^2-F_c^2)2]/\Sigma[w(F_o^2)2]]1/2$.

Table 3
Selected bond lengths (Å) and angles (°) for $[Cu_2Mo_4O_{13}(3,3'\text{-bipy})_2]\cdot H_2O$ ($\mathbf{1}\cdot H_2O$)

Bond lengths	
Cu(1)–N(2)	1.924(7)
Cu(1)–N(1)	1.931(7)
Cu(1)–O(8)	2.186(5)
Mo(1)–O(1)	1.681(8)
Mo(1)–O(2)	1.755(8)
Mo(1)–O(9)#1	1.955(5)
Mo(1)–O(9)	1.955(5)
Mo(1)–O(3)	2.126(7)
Mo(1)–O(3)#2	2.377(7)
Mo(1)–Mo(3)#1	3.2143(11)
Mo(2)–O(5)	1.692(8)
Mo(2)–O(4)	1.714(8)
Mo(2)–O(6)	1.927(5)
Mo(2)–O(6)#1	1.927(5)
Mo(2)–O(2)#2	2.274(8)
Mo(2)–O(3)	2.448(7)
Mo(3)–O(7)	1.688(5)
Mo(3)–O(8)	1.721(5)
Mo(3)–O(6)	1.890(5)
Mo(3)–O(9)	1.998(5)
Mo(3)–O(9)#3	2.314(5)
Mo(3)–O(3)	2.3243(12)
Bond angles	
N(2)–Cu(1)–N(1)	156.2(3)
N(2)–Cu(1)–O(8)	101.6(3)
N(1)–Cu(1)–O(8)	101.3(3)
O(1)–Mo(1)–O(2)	105.2(4)
O(1)–Mo(1)–O(9)	101.96(16)
O(2)–Mo(1)–O(9)	95.95(17)
O(9)#1–Mo(1)–O(9)	149.4(3)
O(1)–Mo(1)–O(3)	99.9(3)
O(2)–Mo(1)–O(3)	154.9(3)
O(9)–Mo(1)–O(3)	78.65(15)
O(1)–Mo(1)–O(3)#2	174.8(3)
O(2)–Mo(1)–O(3)#2	79.9(3)
O(9)–Mo(1)–O(3)#2	77.23(16)
O(3)–Mo(1)–O(3)#2	75.0(3)
C(5)–N(1)–Cu(1)	119.3(6)
C(1)–N(1)–Cu(1)	122.3(6)
C(6)–N(2)–Cu(1)	118.3(6)
C(10)–N(2)–Cu(1)	125.0(6)

Symmetry transformations used to generate equivalent atoms: #1 x, $-y+1$, z; #2 $-x$, $-y+1$, $-z$; #3 $-x$, y, $-z$; #4 $x+1/2$, $-y+1/2$, $z+1$; #5 $x-1/2$, $-y+1/2$, $z-1$.

Table 4
Selected bond lengths (Å) and angles (°) for $[CuMo_4O_{13}(Hdipyreth)]$ (**2**)

Bond lengths	
Cu(1)–N(1)	1.935(6)
Cu(1)–O(1)	1.980(5)
Cu(1)–O(5)#1	2.026(5)
Cu(1)–O(13)	2.067(5)
O(5)–Cu(1)#1	2.026(5)
Bond angles	
N(1)–Cu(1)–O(1)	132.3(2)
N(1)–Cu(1)–O(5)#1	122.2(2)
O(1)–Cu(1)–O(5)#1	95.6(2)
N(1)–Cu(1)–O(13)	106.8(2)
O(1)–Cu(1)–O(13)	103.0(2)
O(5)#1–Cu(1)–O(13)	86.7(2)
Mo(1)–O(1)–Cu(1)	142.3(3)
Mo(2)–O(5)–Cu(1)#1	135.9(3)
Mo(4)–O(13)–Cu(1)	135.5(3)
C(1)–N(1)–Cu(1)	115.9(5)
C(5)–N(1)–Cu(1)	125.2(5)

Symmetry transformations used to generate equivalent atoms: #1 $-x+2$, $-y+1$, $-z+1$; #2 $-x+1$, $-y+1$, $-z+1$.

kinetic phases, rather than the thermodynamic phase are most likely isolated [22,23].

Six isomeric forms of octamolybdate, $[Mo_8O_{26}]^{4-}$, have been described. The α- and β- forms are selectively crystallized from aqueous solutions of molybdate acidified to pH 3–4, followed by addition of the appropriate cations [24–26]. More recently, the γ-isomer has been prepared from aqueous solution by appropriate choice of cations [27,28]. The δ-form has been isolated by both conventional and hydrothermal crystallization [11,29]. The ε and ξ-isomer have to date only been observed in the products of hydrothermal reactions [11,30].

As summarized in Table 1, the structures of the various octamolybdate isomers differ in the types of polyhedra which fuse to form the cluster and in the linkages between polyhedra. The most common, and compact, of the octamolybdate structures is that observed for β-$Mo_8O_{26}^{4-}$, which exhibits eight edge-sharing octahedra, while the ε-form possesses the most open ellipsoidal structure.

Employing a small dipodal linear ligand, namely 3,3′-bipyridine, the compound $[Cu_2Mo_4O_{13}(3,3'\text{-bipy})_2]\cdot H_2O$ ($\mathbf{1}\cdot H_2O$) was synthesized by hydrothermal methods. The structure of $\mathbf{1}\cdot H_2O$ is constructed from the common β-$\{Mo_8O_{26}\}^{4-}$ octamolybdate cluster capped on four sites by trigonal planar Cu(I) sites, each of which bond to two nitrogen donors of the 3,3′-bipy ligand and one oxo-group of the $\{MoO_6\}$ octahedra to form four $\{CuN_2O\}^{1-}$ sub-units. As shown in Fig. 1, the $\{Cu(bipy)\}_n^{n+}$ substructure propagates as a one-dimensional chain. Adjacent chains are connected through the $\{Mo_8O_{26}\}^{4-}$ building blocks to form an overall two-dimensional network with the cavities filled by interstitial water molecules of crystallization. The capping of the two adjacent Mo octahedral at two termini of the cluster shown in Fig. 2 results in an unusual parallel, double chain Cu-ligand substructure and the presence of a bimetallic $\{Cu_4Mo_8O_{26}\}$ neutral cluster building block.

As shown in Fig. 3 the structure of $[CuMo_4O_{13}(Hdipyreth)]$ (**2**) may be described as a ribbon of edge- and corner-sharing $\{MoO_6\}$ octahedra, decorated with peripheral $\{Cu(Hdipyreth)O_3\}$ tetrahedra. The ligand has a pendant pyridyl arm that is protonated in order to

Table 5
Selected bond lengths (Å) and angles (°) for $[Cu(dpp)]_2[Cu_2(\alpha\text{-}Mo_8O_{26})(dpp)_2]\cdot 2H_2O$ (**3**·$2H_2O$)

Bond lengths	
Cu(1)–N(1)	1.907(10)
Cu(1)–N(2)	1.912(10)
Cu(1)–Cu(1)#1	3.043(3)
Cu(2)–N(4)	1.909(10)
Cu(2)–N(3)	1.910(10)
Mo(1)–O(3)	1.719(7)
Mo(1)–O(1)	1.785(7)
Mo(1)–O(4)	1.788(8)
Mo(1)–O(2)	1.793(7)
Mo(2)–O(8)	1.702(7)
Mo(2)–O(9)	1.710(8)
Mo(2)–O(10)	1.911(7)
Mo(2)–O(7)	1.921(7)
Mo(2)–O(2)#2	2.412(7)
Mo(2)–O(4)	2.438(7)
Mo(3)–O(11)	1.697(8)
Mo(3)–O(13)	1.699(7)
Mo(3)–O(10)	1.910(7)
Mo(3)–O(12)	1.912(7)
Mo(3)–O(2)#2	2.389(8)
Mo(4)–O(6)	1.695(8)
Mo(4)–O(5)	1.706(7)
Mo(4)–O(7)	1.902(7)
Mo(4)–O(12)#2	1.905(7)
Mo(4)–O(1)#2	2.366(7)
Mo(4)–O(4)	2.386(8)
Bond angles	
N(1)–Cu(1)–N(2)	163.8(4)
N(1)–Cu(1)–Cu(1)#1	99.2(3)
N(2)–Cu(1)–Cu(1)#1	94.9(3)
N(4)–Cu(2)–N(3)	174.2(4)
C(10)–N(2)–Cu(1)	124.4(8)
C(6)–N(2)–Cu(1)	118.3(8)
C(18)–N(3)–Cu(2)	121.4(8)
C(13)–N(3)–Cu(2)	120.3(8)
C(23)–N(4)–Cu(2)	120.0(8)
C(19)–N(4)–Cu(2)	122.4(8)

Symmetry transformations used to generate equivalent atoms: #1 $-x+1, -y, -z+1$; #2 $-x+1, -y+1, -z+1$; #3 $x, y, z+1$; #4 $-x+2, -y+1, -z+1$; #5 $x, y, z-1$.

charge balance the overall structure. The coordination geometry at the Cu(I) site is defined by an apical nitrogen atom, with the basal plane generated by the oxygen donors of the three oxo-groups from three molybdenum sites. The puckering of the molybdate chain provides the surface cavities which accommodate the tetrahedral Cu(I) sites. The molybdate ribbon appears as a stepped chain in profile and may be considered to be constructed from octamolybdate units fused at two oxo-groups, as shown in Fig. 4(a). The octamolybdate subunits may in turn be described as two groups of *cis*-edge-sharing tetranuclear units fused through edge-sharing to generate the distinctive step projection of the ribbon. Removal of the oxo-groups contributed by the adjacent octamolybdate subunits reveals that the building block of the ribbon is the γ-octamolybdate, shown in Fig. 4(b). The γ-octamolybdate cluster has been described previously as a discrete building block in the copper molybdate species $[\{Cu(en)_2\}_2Mo_8O_{26}]$ [31] and $[\{Cu(pyridazine)\}_4H_4Mo_8O_{26}]$ [32]. It is tempting to speculate that, under the hydrothermal conditions used for the preparation of **2**, there is structural preassembly of the octamolybdate substructure followed by fusion into the ribbon structure. However, the evidence for such preassembly remains indirect. On the other hand, the influence of templating components is well-established, suggesting that the $\{Cu(Hdipyreth)\}_n^{n+}$ coordination cation is a structural determinant under these conditions.

The larger and more flexible ligand 4,4′-trimethylenedipyridine (dpp) has yielded another new compound based on the octamolybdate family of compounds. The structure of **3**·$2H_2O$ is constructed from the α-octamolybdate isomer and two distinct Cu(I) centers, exhibiting different geometries and unique ligand orientations.

As shown in Fig. 5 the structure of **3**·$2H_2O$ is composed of molybdate clusters linked to each other via two edge sharing tetrahedral Cu(I) centers on the apical $\{MoO_4\}$ tetrahedra of each to form a one-dimensional chain. The periphery of the cluster is decorated with trigonal planar Cu(I) sites that bond to the dpp ligand in a one-dimensional chain to propagate the structure as a two-dimensional slab. Water molecules of crystallization occupy the interlamellar regions of the structure. The edge sharing Cu(I) tetrahedral centers are in turn bound to two dpp ligands which bridge the two Cu(I) tetrahedra. The nitrogen donors of the dpp ligand occupy one position in the basal plane of one Cu(I) center and the apical position of the second Cu(I) tetrahedra to wrap the two ligands into a box around the Cu(I) centers. This connectivity in turn orients the dpp ligand parallel with the $\{Cu_4(Mo_8O_{26})\}$ oxide chain shown in Fig. 6. The second Cu(I) center is trigonal planar and extends from the peripheral octahedral Mo sites of the α-octamolybdate cluster. These edge-sharing trigonal planar Cu(I) sites are bound to transannular $\{MoO_6\}$ octahedra with one Cu(I) site directed above and one Cu(I) site directed below the $\{Mo_6O_{24}\}$ ring. The consequence of this is to form parallel $\{Cu(I)(dpp)\}_n^{n+}$ infinite chains at two points of attachment to the α-octamolybdate clusters. The net result is a one-dimensional ladder motif, with the $\{Cu(dpp)\}_n^{n+}$ chains serving as the rails and the molybdate clusters as the rungs. These chains are in turn linked through the tetrahedral Cu(I) sites into a two-dimensional structure as shown in Fig. 7. The flexibility of the propylene tether of the dpp ligand is evident in the two distinct Cu(I)–dpp substructures. In one case the tether extends to permit extension in a one-dimensional chain, while in the second instance, the

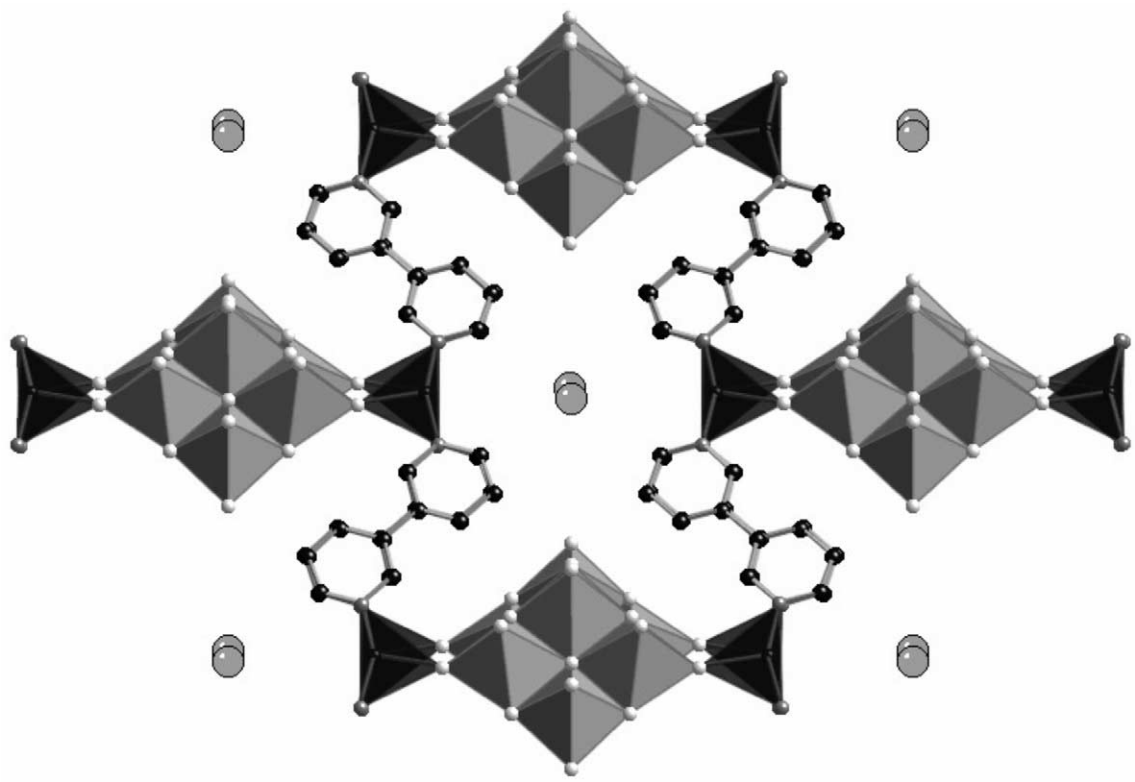

Fig. 1. A polyhedral and ball and stick representation of the structure of $[Cu_2Mo_4O_{13}(3,3'\text{-bipy})_2]\cdot H_2O$.

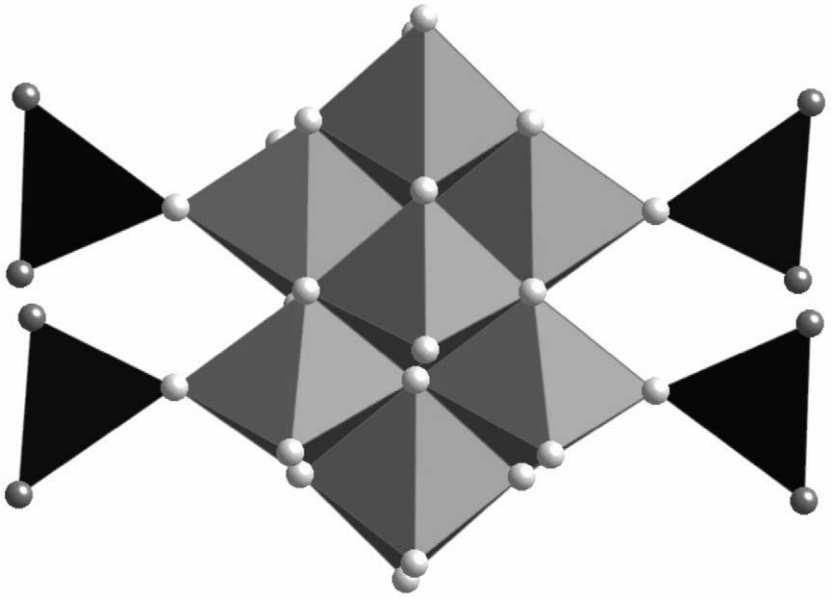

Fig. 2. A view of the β-octamolybdate capped by four Cu(I) centers in the structure of $[Cu_2Mo_4O_{13}(3,3'\text{-bipy})_2]\cdot H_2O$.

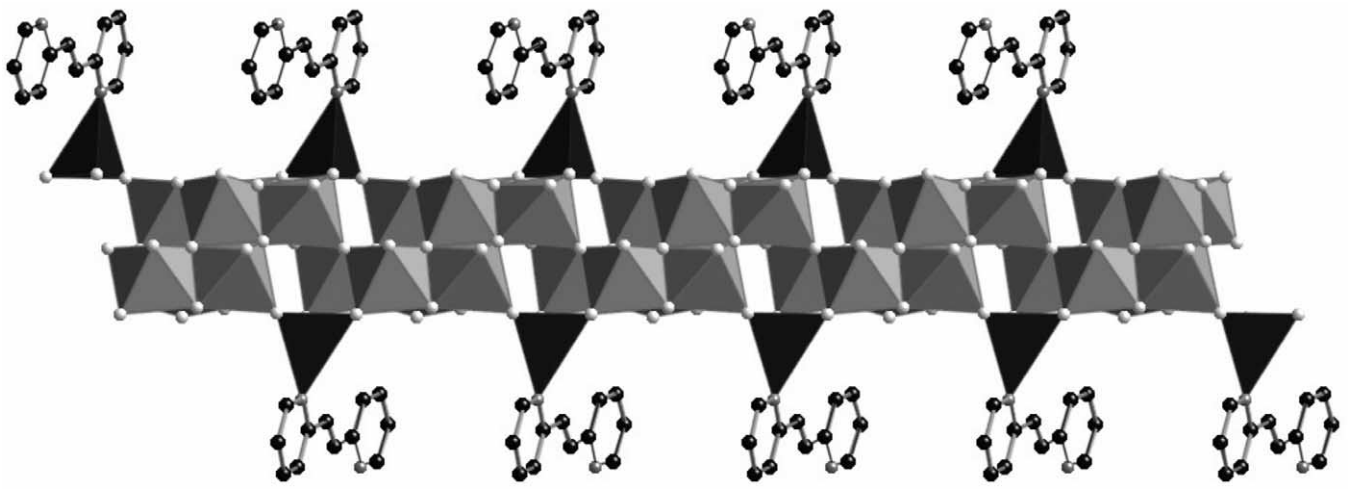

Fig. 3. A polyhedral and ball and stick representation of the structure of $[CuMo_4O_{13}(Hdipyreth)]$.

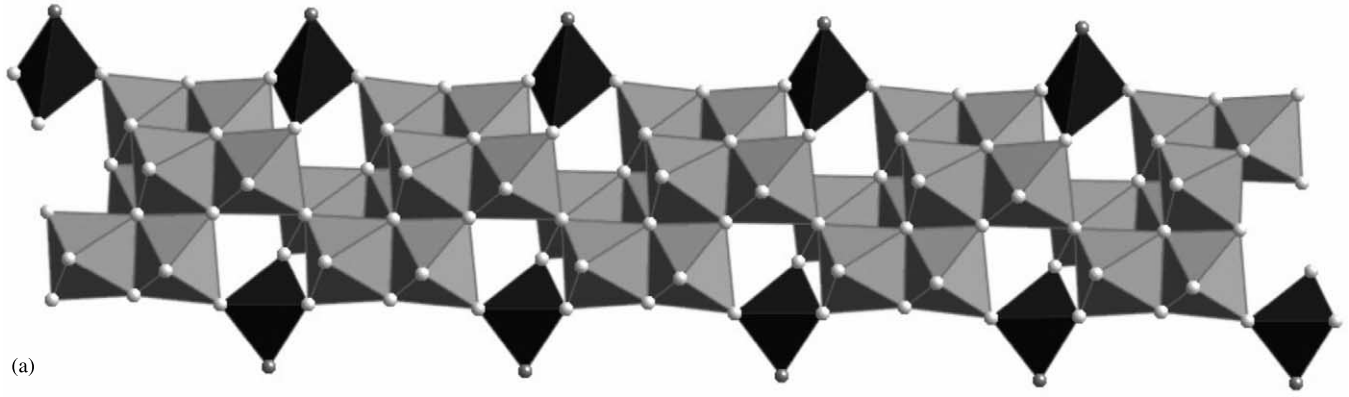

(a)

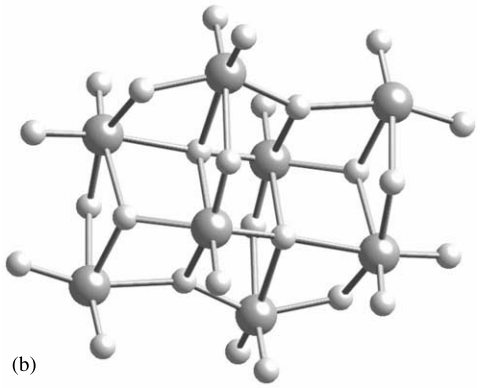

(b)

Fig. 4. The mixed metal oxide chain of the structure of $[CuMo_4O_{13}(Hdipyreth)]$. A ball and stick view of the γ-$[Mo_8O_{26}]^{4-}$ cluster embedded in the molybdate chain of **2**.

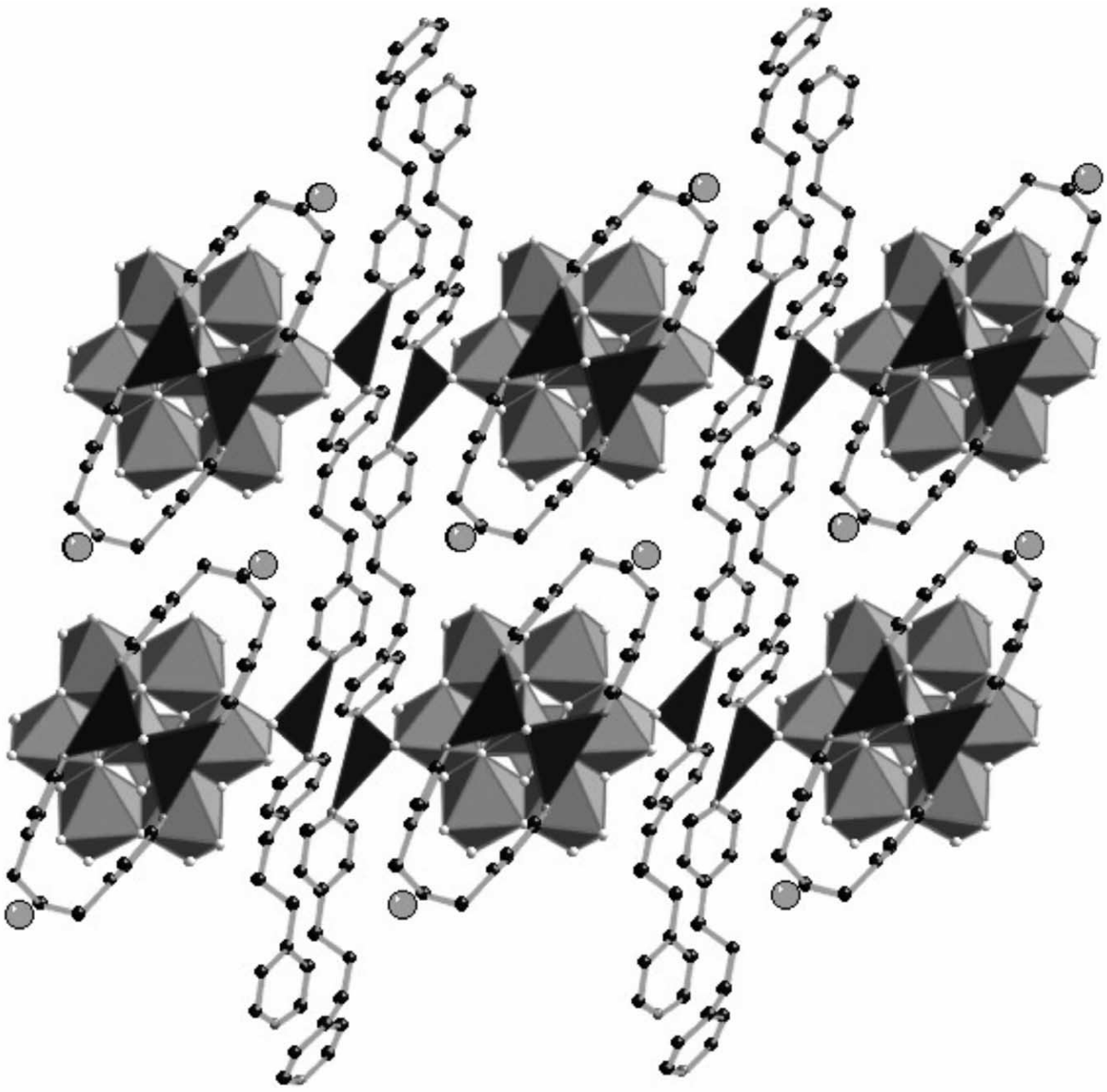

Fig. 5. A polyhedral and ball and stick representation of the structure of $[Cu(dpp)]_2[Cu_2(\alpha\text{-}Mo_8O_{26})(dpp)_2]\cdot 2H_2O$.

tether folds to provide a clothespin ligand geometry, which results in the binuclear $\{Cu_2(dpp)_2\}^{2+}$ subunit.

The α-isomer of the molybdate substructure has been previously described in $[\{Cu(bpe)\}_4(\alpha\text{-}Mo_8O_{26})]\cdot 2H_2O$ [32]. The cluster is constructed from edge- and corner-sharing of six $\{MoO_6\}$ octahedra and two $\{MoO_4\}$ tetrahedra. The overall cluster geometry may be described as six edge-sharing $\{MoO_6\}$ octahedra compromising the equatorial ring capped on both poles by corner-sharing $\{MoO_4\}$ tetrahedra. Consequently, each $\{MoO_6\}$ octahedron engages in an edge-sharing interaction with an adjacent octahedron, along with corner-sharing interactions with two capping tetrahedron. The capping tetrahedra participate in three corner-sharing interactions with the octahedral sites to leave a single terminal oxo-group. The three bridging oxo-groups engage in μ_2-bridging between the edge-sharing sets of octahedra.

4. Conclusions

Hydrothermal techniques have been exploited in the synthesis of three new compounds based on the octa-

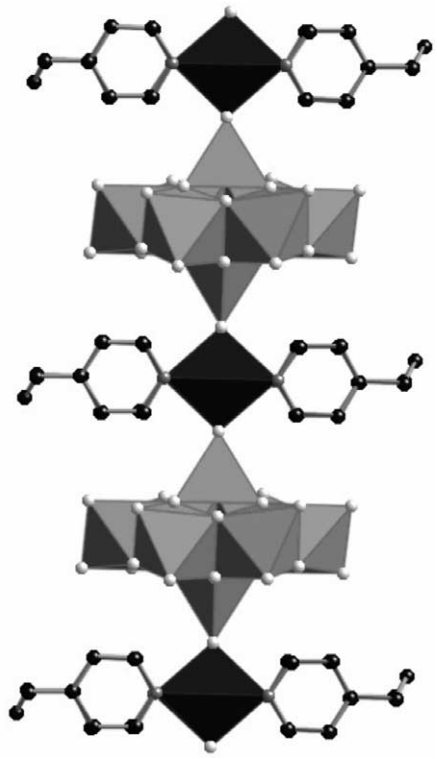

Fig. 6. A view of the chain structure with the dpp ligand parallel with the $\{Cu_4(Mo_8O_{26})\}$ oxide chain.

molybdate family of compounds. The richness and diversity of the chemistry has allowed the isolation of both one and two-dimensional structures, incorporating molybdate substructures ranging from the most compact β-octamolybdate cluster to a more open-framework α-octamolybdate cluster and in one case to a fused γ-octamolydate sub-structure. The differing lengths of ligands and varied donor dispositions together with the coordination preference of the secondary metal are structural determinants, although other factors in the complex hydrothermal reaction domain also exert some influence on the structural outcome.

5. Supplementary materials

The supplementary materials, including atomic positional parameters, hydrogen atom positions, anisotropic thermal parameters and full tables of bond lengths and angles have been deposited with the Cambridge Crystallographic Data Centre, 12 Union Road, Cambridge, CB2 IEZ, UK (fax: +44-1223-336033; e-mail: deposit@ccdc.cam.ac.uk or www: http://www.ccdc.cam.ac.uk), as supplementary material Nos. 194774–194776 and can be obtained by contacting the CCDC, quoting the article details and the corresponding SUP number.

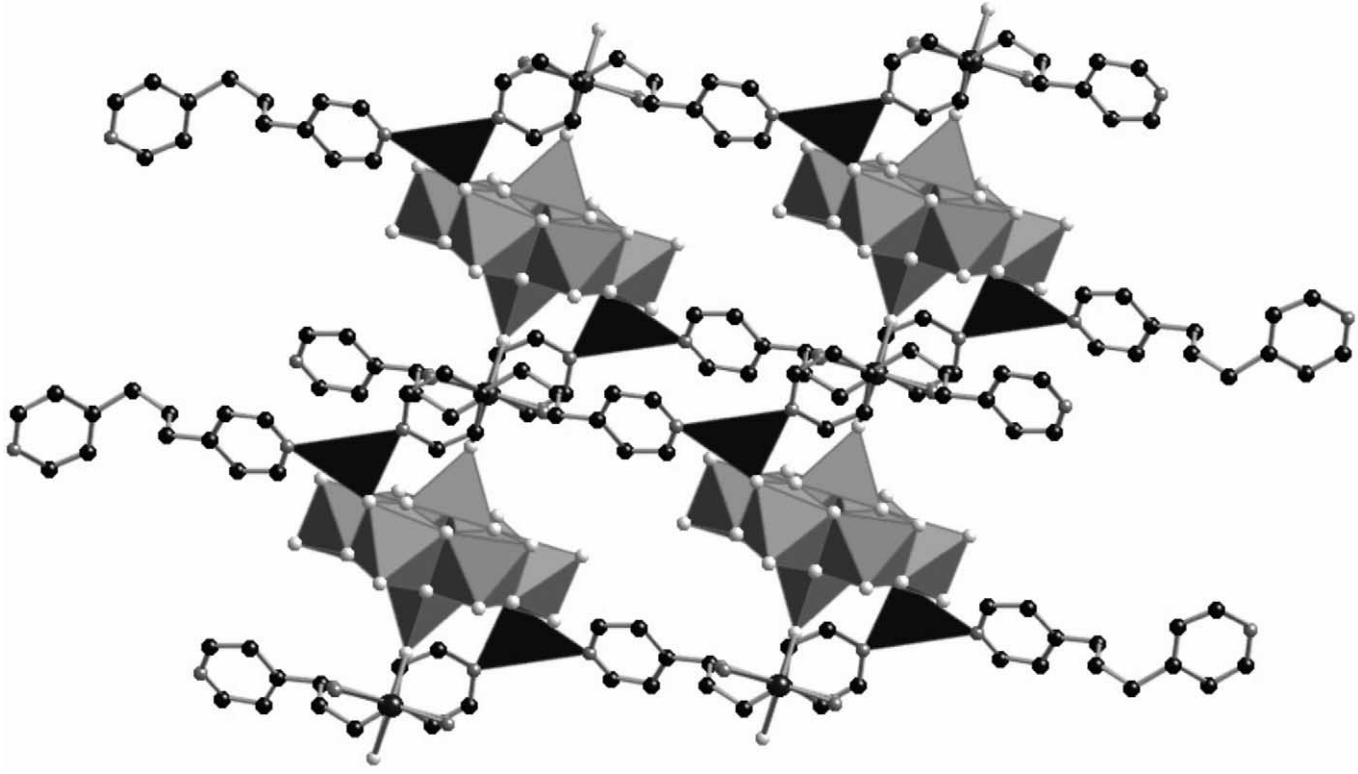

Fig. 7. A view of the ladder motif of structure $\mathbf{3}\cdot 2H_2O$.

Acknowledgements

This work was supported by grant CHE 9987471 from the National Science Foundation.

References

[1] (a) See for example: S. Lopez, M. Kahrman, M. Harmoto, S.W. Keller, Inorg. Chem. 36 (1997) 6138 and references therein;
(b) B.F. Hoskins, R. Robson, S1IZ45, D.A. Angew. Chem., Int. Ed. Engl. 36 (1997) 2336;
(c) M.A. Withersby, A.J. Blake, N.R. Champness, P. Hubberstey, W.S. Li, M. Schröder, Angew. Chem., Int. Ed. Engl. 36 (1997) 972;
(d) O.M. Yaghi, H. Li, T.L. Groy, Inorg. Chem. 36 (1997) 4292;;
(e) L. Carlucci, G. Giani, D.W. v. Gudenberg, D.M. Proserpio, Inorg. Chem. 36 (1997) 3812.

[2] T.E. Mallouk, H.J. Stein, J. Chem. Educ. 67 (1990) 829.

[3] D. Hagrman, P.J. Zapf, J. Zubieta, Angew. Chem., Int. Ed. Engl. 38 (1999) 2798 (and references therein).

[4] M.-L. Tong, S.-M. Chen, B.-H. Ye, S.W. Ng, Inorg. Chem. 37 (1998) 5278.

[5] (a) See for example: L. Carlucci, G. Ciani, D.M. Proserpio, A. Sironi, J. Chem. Soc., Dalton Trans. (1997) 1801;
(b) A.S. Batsanov, M.J. Begley, P. Hubberstey, J. Stroud, J. Chem. Soc., Dalton Trans. (1996) 1947;
(c) P. Losier, M.J. Zaworotko, Angew. Chem., Int. Ed. Engl. 35 (1996) 2779;
(d) O.M. Yaghi, H. Li, T.L. Groy, Inorg. Chem. 36 (1997) 4292;
(e) M. Fujita, Y.J. Kwon, S. Washizu, K. Ogura, J. Am. Chem. Soc. 116 (1994) 1151;
(f) A.J. Blake, N.R. Champness, S.S.M. Chung, W.-S. Li, M. Schröder, Chem. Commun. (1997) 1675;
(g) S.W. Keller, Angew. Chem., Int. Ed. Engl. 36 (1997) 247.

[6] (a) In the case of 4,4′-bpy as the bridging ligand, see for example: A.J. Blake, S.J. Hill, P. Hubberstey, W.-S. Li, J. Chem. Soc., Dalton Trans. (1997) 913;
(b)) N. Masciocchi, P. Cairati, L. Carlucci, G. Mezza, G. Ciani, A. Sironi, J. Chem. Soc., Dalton Trans. (1996) 2739;
(c) F. Robinson, M.J. Zaworotko, J. Chem. Soc., Chem. Commun. (1995) 2413;
(d) O.M. Yaghi, H. Li, J. Am. Chem. Soc. 118 (1996) 295;
(e) D. Hagrman, R.P. Hammond, R.C. Haushalter, J. Zubieta, Chem. Mater. 10 (1998) 2091;
(f) A.J. Blake, S.J. Hill, P. Hubberstey, W.-S. Li, J. Chem. Soc., Dalton Trans. (1998) 909;
(g) R.W. Gable, B.F. Hoskins, R. Robson, J. Chem. Soc., Chem. Commun. (1990) 1677;
(h) S. Subramanian, M.J. Zaworotko, Angew. Chem., Int. Ed. Engl. 34 (1995) 2127;
(i) J. Li, H. Zeng, J. Chen, Q. Wang, X. Wu, Chem. Commun. (1997) 1213;
(j) M. Kondo, T. Yoshitomi, K. Seki, H. Matsuzaka, S. Kitagawa, Angew. Chem., Int. Ed. Engl. 36 (1997) 1725;
(k) O.M. Yaghi, G. Li, Angew. Chem., Int. Ed. Engl. 34 (1995) 207;
(l) M.-L. Tong, B.-H. Ye, J.-W. Cai, X.-M. Chen, S.W. Ng, Inorg. Chem. Commun. (1994) 2755;
(m) L.R. MacGillivray, S. Subramanian, M.J. Zaworotko, J. Chem. Soc., Chem. Commun. (1994) 1325.

[7] (a) For tethered bipyridine type ($NC_5H_4–X–C_5H_4N$), see for example: A.J. Blake, N.R. Champness, A. Kholobystov, D.A. Lemenovskii, W.-S. Li, M. Schröder, Chem. Commun. (1997) 2027;
(b) Y.J. Fujita, O. Kwon, K. Sasaki, K. Yamaguchi, K. Ogura, J. Am. Chem. Soc. 117 (1995) 7287;
(c) L. Carlucci, G. Ciani, D.W. v. Gudenberg, D.M. Proserpio, Inorg. Chem. 36 (1997) 3812;
(d) M. Fujita, Y.J. Kwon, M. Miyazawa, K. Ogura, J. Chem. Soc., Chem. Commun. (1994) 1977;
(e) L. Carlucci, G. Ciani, P. Macchi, D.M. Proserpio, Chem. Commun. (1998) 1837;
(f) M.A. Withersby, A.J. Blake, N.R. Champness, P. Hubberstey, W.-S. Li, M. Schröder, Angew. Chem., Int. Ed. Engl. 36 (1997) 232;
(g) M.J. Hannon, C.L. Painting, W. Errington, Chem. Commun. (1997) 1805;
(h) A. Neels, H. Stoeckli-Evans, A. Escuer, R. Vicente, Inorg. Chem. 34 (1995) 1946;
(i) C.L. Schauer, E. Matwey, F.W. Fowler, J.W. Lauher, J. Am. Chem. Soc. 119 (1997) 10245;
(j) K.N. Power, T.L. Hennigar, M.J. Zaworotko, Chem. Commun. (1998) 595;
(k) A.J. Blake, N.R. Champness, S.S.M. Chung, W.-S. Li, M. Schröder, Chem. Commun. (1997) 1005;
(l) A.J. Blake, N.R. Champness, A.N. Khlobystov, D.A. Lemenovskii, W.-S. Li, M. Schröder, Chem. Commun. (1997) 1339.

[8] D.J. Chesnut, D. Hagrman, P.J. Zapf, R.P. Hammond, R. LaDuca, Jr., R.C. Haushalter, J. Zubieta, Coord. Chem. Rev. 190–192 (1999) 737.

[9] D. Hagrman, P.J. Hagrman, J. Zubieta, Comments Inorg. Chem. 21 (1999) 225.

[10] D. Hagrman, J. Zubieta, ACA Trans. 33 (1998) 105.

[11] D. Hagrman, C. Zubieta, R.C. Haushalter, J. Zubieta, J. Angew. Chem., Int. Ed. Engl. 36 (1997) 873.

[12] A. Kitamura, T. Ozeki, A. Yagasaki, Inorg. Chem. 36 (1997) 4270.

[13] E.K. Andersen, J. Villadsen, Acta Chim. Scand. 47 (1993) 748.

[14] (a) M.I. Khan, E. Yohannes, D. Powell, Chem. Commun. (1999) 23;
(b) J.R. Galán-Mascarós, C. Gimenéz-Saiz, S. Triki, C.J. Gómez-Garcia, E. Coronado, L. Ouahab, Angew. Chem., Int. Ed. Engl. 34 (1995) 1460;
(c) A. Kitamura, T. Ozeki, A. Yagasaki, Inorg. Chem. 36 (1997) 4275;
(d) J. Lu, Y. Xu, N.K. Gok, L.S. Chia, Chem. Commun. (1998) 379;
(e) M.I. Khan, E. Yohannes, R.J. Doldens, Angew. Chem., Int. Ed. Engl. 38 (1999) 1292.

[15] A. Müller, S.Q.N. Shah, H. Bögge, M. Schmidtmann, Nature 397 (1999) 49.

[16] Siemens, 'SMART Software Reference Manual' Siemens Analytical X-ray Instruments, Inc., Madison, WI, 1994.

[17] G.M. Sheldrick, SADABS: Program for Empirical Absorption Corrections, University of Göttingen, Germany, 1996.

[18] G.M. Sheldrick, SHELXL-96. Program for the Refinement of Crystal Structures, University of Göttingen, Germany, 1996.

[19] R.M. Barrer, Hydrothermal Chemistry of Zeolites, Academic Press, New York, 1982.

[20] R.C. Haushalter, L.A. Mondi, Chem. Mater. 4 (1982) 31, and references therein.

[21] M.I. Khan, J. Zubieta, Prog. Inorg. Chem. 43 (1995) 1 (and references therein).

[22] A. Stein, S.W. Keller, T.G. Mallouk, Science 259 (1993) 1558.

[23] J. Gopalakrishnan, Chem. Mater. 7 (1995) 1265.

[24] K.H. Tytko, Z. Naturforsch., Teil B B31 (1976) 757.

[25] A.F. Masters, S.F. Ghellu, R.T. Brownlee, M.J. O'Connor, A.G. Wedd, Inorg. Chem. 19 (1980) 3866.

[26] M.T. Pope, Proj. Inorg. Chem. 39 (1991) 255.

[27] M.L. Niven, J.J. Cruywagen, J.B.B. Heyns, J. Chem. Soc., Dalton Trans. (1991) 2007.

[28] M. Inoue, T. Yamase, Bull. Chem. Soc. Jpn. 68 (1995) 3055.
[29] R. Xi, B. Wang, K. Isobe, T. Nishioka, K. Toriumi, Y. Ozawa, Inorg. Chem. 33 (1994) 833.
[30] J.-Q. Xu, R.-Z. Wang, G.-Y. Yang, Y.-H. Xing, D.-M. Li, W.-M. Bu, L. Ye, Y.-G. Fan, G.-D. Yang, Y. Xing, Y.-H. Lin, H.-Q. Jia, Chem. Commun. (1999) 983.
[31] J.R.D. DeBord, R.C. Haushalter, T.M. Meyer, D.J. Rose, P.J. Zapf, J. Zubieta, Inorg. Chim. Acta 256 (1997) 165.
[32] D. Hagrman, C. Sangregorio, C.J. O'Connor, J. Zubieta, J. Chem. Soc., Dalton Trans. (1998) 3707.